

## Electron glass in samples approaching the mesoscopic regime

V. Orlyanchik and Z. Ovadyahu

*Racah Institute of Physics, The Hebrew University, Jerusalem 91904, Israel*

(Received 28 February 2007; published 15 May 2007)

We study the dependence of the glassy properties of strongly localized  $\text{In}_2\text{O}_{3-x}$  films on the sample lateral dimensions. Characteristic mesoscopic effects such as reproducible conductance fluctuations (CFs) are readily observable in gated structures for sample size smaller than  $100\ \mu\text{m}$  measured at 4 K, and the relative amplitude of the CF decreases with the sample volume as does the flicker noise. By contrast, down to sample size of a few microns, the nonequilibrium features that are attributed to the electron glass are indistinguishable from those observed in macroscopic samples, and in particular, the relaxation dynamics is independent of sample size down to  $2\ \mu\text{m}$ . In addition, the usual features that characterize the electron glass including slow relaxation, memory effects, and full-aging behavior are all observed in the “mesoscopic” regime, and they appear to be independent of the conductance fluctuations.

DOI: [10.1103/PhysRevB.75.174205](https://doi.org/10.1103/PhysRevB.75.174205)

PACS number(s): 71.55.Jv, 73.23.-b, 72.70.+m, 73.61.Jc

### I. INTRODUCTION

Nonergodic transport properties of Anderson insulators have been reported in a number of systems studied at low temperatures.<sup>1-4</sup> When excited from equilibrium by, e.g., a sudden change of a gate voltage, the conductance of the system increases, and this excess conductance  $\Delta G$  persists for long times (in some cases, days) after the excitation. Vaknin *et al.*<sup>5</sup> argued that such extended relaxation times as well as various memory effects exhibited by these systems are difficult to explain unless electron-electron correlations play a decisive role.<sup>6</sup> For a medium that lacks metallic screening, it is natural to assume that the Coulomb interaction is relevant. This point of view was indeed taken in some theoretical models where the long-range nature of the Coulomb interaction was used to justify a mean-field treatment.<sup>7</sup>

In this work, we explore the behavior the electron glass when the system size approaches the mesoscopic regime of hopping conductance. The study is motivated by two main reasons. One goal is to assess the spatial range of correlation in the electron glass by monitoring the dynamics as function of system size (which seems a viable approach when dealing with a long-range interaction such as the unscreened Coulomb potential). This is based on the notion that the slow relaxation is presumably a result of a many-particle scenario,<sup>6,8</sup> and therefore the dynamics should become size dependent below a certain scale.<sup>9</sup> Another reason to study small systems is that it should shed light on the interplay between the electron slow dynamics and the ionic one which may be reflected in the temporal aspect of some specific mesoscopic effects.

Our main finding is that at least down to sample size  $L$  of a few microns, the basic electron-glass properties, namely, slow relaxation, memory, and aging, remain essentially the same as in macroscopic samples. In particular, the characteristic relaxation time, observable in relaxation experiments of  $\Delta G$ , shows no scale dependence when the sample size is changed from millimeters down to  $2\ \mu\text{m}$ .

At liquid-helium temperatures, samples with  $L \leq 100\ \mu\text{m}$  exhibit reproducible conductance fluctuation (CF) as function of the chemical potential. These are observable in

the conductance versus gate voltage  $G(V_g)$  scans as a fluctuating component of  $G$ , defining a sample-specific pattern that changes form when the sample is thermally recycled. The CF pattern appears whether or not the underlying glassy system was allowed to equilibrate prior to taking a  $G(V_g)$  sweep. A  $G(V_g)$  scan taken after the sample equilibrates reveals the usual memory cusp, which is the main earmark of the electron glass,<sup>1,4-6</sup> while the CF appears just as a superimposed structure with no sign of intermodulation effects. The two types of conductance modulation observable in the  $G(V_g)$  scans, namely, the CF and memory cusp, are shown to be distinct physical phenomena; they are associated with different spatial scales and quite different time scales.

### II. EXPERIMENT

#### A. Sample preparation and measurement techniques

The  $\text{In}_2\text{O}_{3-x}$  films used in this work were e-gun evaporated on a  $\text{SiO}_2$  insulating layer ( $0.5\ \mu\text{m}$  thick) thermally grown on a  $\langle 100 \rangle$  Si wafer. The choice of  $\text{In}_2\text{O}_{3-x}$ , the crystalline version of indium oxide for this study, was motivated by its essentially constant stoichiometry (due to crystal chemistry constraints) hence a fairly constant carrier concentration. As was shown previously using the amorphous version, a change in carrier concentration may lead to a large variance in the glassy features,<sup>6</sup> which might mask the size dependence. The Si wafer was boron doped and had resistivity of  $2 \times 10^{-3}\ \Omega\ \text{cm}$ , deep in the degenerate regime. It could thus be used as an equipotential gate electrode for a low-temperature measurement where the  $\text{In}_2\text{O}_{3-x}$  served as the active layer in a three-terminal device. Lateral dimensions of the samples were controlled using a stainless-steel mask (for samples larger than  $0.5\ \text{mm}$ ), optical lithography (for sizes in the range  $30\text{--}200\ \mu\text{m}$ ), or e-beam lithography (for samples smaller than  $30\ \mu\text{m}$ ). Samples used in this study had length  $L$  and width  $W$  that ranged from  $2\ \mu\text{m}$  to  $2\ \text{mm}$  and typical thickness  $d = 55 \pm 5\ \text{\AA}$ . The “source” and “drain” contacts to the  $\text{In}_2\text{O}_{3-x}$  film were made from thermally evaporated  $\approx 500\text{--}\text{\AA}$ -thick gold films. Fuller details of sample preparation and characterization are given elsewhere.<sup>5</sup>

Conductance measurements were performed using two-terminal ac technique, employing ITHACO-1211 current preamplifier and PAR-124A lock-in amplifier. In the metal-oxide-semiconductor-field-effect-transistor-like samples, gate-voltage sweeps were affected by charging a  $10 \mu\text{F}$  capacitor with a constant current source. All the measurements reported here were performed with the samples immersed in liquid helium at  $T=4.11 \text{ K}$  held by a 100 l storage dewar. This allowed long term measurements without disturbing the samples as well as a convenient way to maintain a stable bath temperature. These requirements are of particular importance for studies of glassy systems where sample history may influence time dependent measurements, as was demonstrated in previous studies.<sup>10</sup> Care was taken to use small bias in the conductance measurements to ensure linear-response conditions, and in general that was the case. The only exception is in the  $2 \mu\text{m}$  samples where some deviations from Ohm's law were observable even at the lowest bias we managed to measure with a reasonable signal to noise ratio (see also Ref. 11).

### III. RESULTS AND DISCUSSION

#### A. Conductance fluctuations

The emphasis in this work is the evolution of the glassy features as the size of the system is reduced. These features are observable by performing conductance measurements employing low-frequency techniques, and therefore flicker noise becomes a major problem in reducing the system size. Mesoscopic samples naturally exhibit a larger  $1/f$  noise than macroscopic specimen with similar resistance (and measured at the same temperature). It was shown elsewhere that the  $1/f$ -noise magnitude in these samples scales with the inverse sample volume as expected of independent fluctuators.<sup>11</sup> It turns out that for  $L$  smaller than few microns, the noise overshadows some of the glassy features, which made it difficult to study samples with  $L, W < 2 \mu\text{m}$ . The other feature that becomes progressively more prominent as  $L$  goes smaller is a set sample-specific pattern that modulates the conductance. These CFs are seen in the gate-voltage sweeps  $G(V_g)$ , which is the main method to study the various glassy properties. When the sample size is reduced, the CF, much like the  $1/f$  noise, eventually masks the glassy effects. In this section, we describe the phenomenology of the CF and their relation to the glassy dynamics on one hand and to the  $1/f$  noise on the other hand.

Figure 1 shows  $G(V_g)$  scans for two of the studied samples, illustrating the reproducibility of the CF pattern upon repeated scans [Figs. 1(a) and 1(b)]. There are obviously some deviations from perfect reproducibility, but they are always within the level expected from the observed magnitude of the  $1/f$  noise. (Namely, the deviation, judged by the cross correlation between a traces taken at time  $t_1$  and  $t_2$ , never exceeded the magnitude of the noise estimated at  $[t_2 - t_1]^{-1}$ .) Another general trend is that the relative reproducibility appears to be better the smaller the sample area. The degree of reproducibility was not sensitive to the scan rate of  $V_g$  (tested over the range of  $0.1 - 100 \text{ mV/s}$ ) so we are

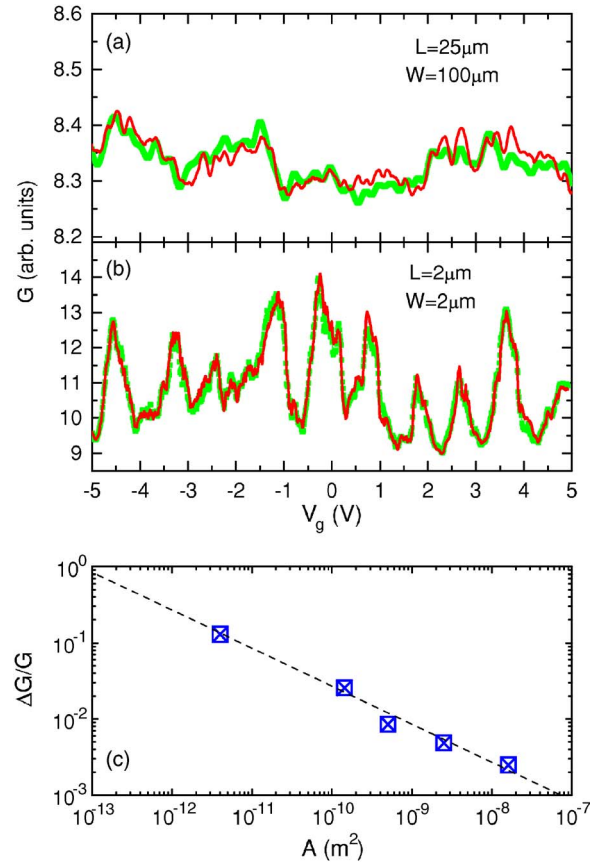


FIG. 1. (Color online)  $G(V_g)$  traces for two of the samples with different sizes. In each case, two traces were taken one after the other starting immediately (within  $\approx 20 \text{ s}$ ) after quench cooling the sample from  $T \approx 50 \text{ K}$  to the measurement temperature of  $4.1 \text{ K}$ . Scan rate was  $10 \text{ mV/s}$ . Sample sheet resistance  $R_{\square} = 57.5$  and  $4 \text{ M}\Omega$  for (a) and (b), respectively. Graph (c) shows the dependence of the rms conductance fluctuations on the sample area. This is based on samples with similar thickness and  $R_{\square}$  (in the range of  $3 - 10 \text{ M}\Omega$ ); each point is the average value of 2–3 samples. The dashed line is a best fit to  $\Delta G/G \propto A^{-1/2}$  law.

inclined to believe that irreproducibility is due to an inherent process, probably related to the  $1/f$  noise.

The relative magnitude of both the CF and the  $1/f$  noise depends on the sample resistance and temperature, as well as on the sample size. The dependence of the rms  $\Delta G$  associated with the CF on the sample area  $A = LW$  for samples with similar resistances and measured at the same temperature is shown in Fig. 1(c) (compare with Fig. 2 in Ref. 11).

The two traces in Fig. 1(a) were taken one after the other starting *immediately* after quench cooling the sample from  $T > 50 \text{ K}$  to  $T = 4.1 \text{ K}$ . Figure 2, on the other hand, shows  $G(V_g)$  traces for a sample taken *after* it was allowed to equilibrate for 12 h with  $V_g$  held at  $V_g^0 = 0 \text{ V}$ . For the second and third quench-cool runs included in the figure, the sample was first warmed up to  $T \approx 70 \text{ K}$ , held there for 10 s, and then quench cooled to  $4 \text{ K}$  and allowed to relax again for 12 h prior to taking a  $G(V_g)$  sweep. In all these instances, the  $G(V_g)$  curves show a “memory cusp” centered at the gate voltage at which the sample equilibrated, in addition to a distinctive set of CF [Fig. 2(a)]. Note that, for each quench,

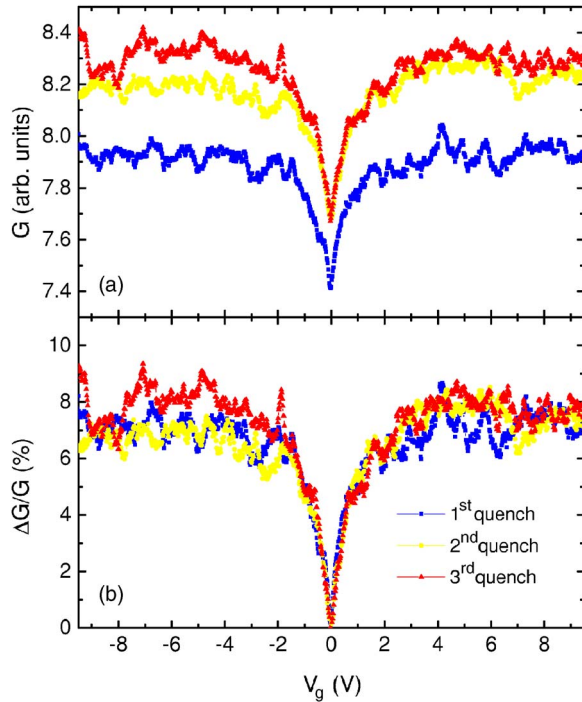


FIG. 2. (Color online) (a)  $G(V_g)$  traces for three consecutive quench-cooling runs of the same sample ( $R_{\square}=57.5$  M $\Omega$ ,  $L=25$   $\mu\text{m}$ ,  $W=100$   $\mu\text{m}$ ). For each trace, the sample was heated to  $\approx 70$  K for 10 s, then cooled to 4 K, and allowed to equilibrate for  $\approx 12$  h, holding  $V_g=0$  V prior to taking a scan (scan rate of 10 mV/s.). Graph (b) is the same data normalized for each run to  $G(0)$ . Note that the memory cusp is nearly identical in all three runs, while the CF pattern is different. Also note that the value of the conductance (that is presumed to reflect the average disorder) is nearly the same in all three quenches (the difference in  $G_0$  between the first and the second quench is negligible with respect to the variation of  $G$  affected by cooling from 70 to 4 K).

a *quench-specific* set of CF is obtained while the average value of  $G$  is nearly identical [Fig. 2(a)], and so is the shape of the associated memory cusp [Fig. 2(b)].

Before discussing the interplay between the CF and the memory cusp, the origin of the CF in these samples needs to be clarified. There is some similarity in behavior between the CF observed in our  $G(V_g)$  and the universal conductance fluctuation (UCF) phenomenon familiar from the weak localization (diffusive) regime.<sup>12</sup> Most notably, the fluctuation pattern produced is like a set of “fingerprints” characteristic of a particular structural, frozen-in configuration. However, the underlying mechanisms for the two phenomena are different. The UCF is a quantum interference effect usually produced by sweeping a magnetic field  $H$  that modulates  $G$  via the Aharonov-Bohm effect (similar behavior has been observed in gate experiments on diffusive samples, likewise related to an interference effect<sup>13</sup>). The CF observed here is associated with a mechanism offered by Lee<sup>14</sup> to account for experiments on quasi-one-dimensional hopping samples.<sup>15</sup> In terms of variable range hopping, our samples are therefore effectively two dimensional (a typical hopping length in our samples at the temperatures used in this work is  $\approx 200$   $\text{\AA}$ ,<sup>16</sup> which is larger than the thickness  $\approx 55$   $\text{\AA}$ ). The underlying

physics of Lee’s mechanism, however, does not depend on the particular dimensionality: The current in hopping systems is carried in a percolation network and controlled by a relatively small number of “critical” or “bottleneck” resistors.<sup>17–19</sup> Like any other resistor in the system, the values of these resistors are given by the Miller-Abrahams expressions<sup>20</sup>  $R_{ij} \propto \exp\left[\frac{2r_{ij}}{\xi} + \frac{|E_i - E_j| + |E_i - \mu| + |E_j - \mu|}{k_B T}\right]$ , where  $r_{ij}$  is the intersite distance in space,  $\xi$  is the localization length,  $E_i$ ,  $E_j$  are the site energies, and  $\mu$  is the chemical potential. Therefore, the actual resistance of these circuit elements depends (among other things) on the value of the chemical potential. Sweeping the gate voltage causes the chemical potential to change, thereby reshuffling the values of the resistors in the system. The CF pattern in this picture reflects the process by which some critical resistors in the percolation network are replaced by other critical resistors as the chemical potential is varied.<sup>14</sup> The fact that by going back and forth with  $V_g$  the pattern reproduces itself suggests that there is an underlying backbone structure of sites that are fairly stable, most likely the positions of the ions that control the disorder in the system. This is the analog of the distribution of scattering centers that determine the magnetic fingerprints in the UCF effect. In both phenomena, the underlying structure changes upon thermal recycling, and in both, the deviations from perfect reproducibility are associated with nonstationary potential disorder which in turn is believed to be the main cause of the  $1/f$  noise.<sup>21</sup>

The relative magnitude of the CF for a given two-dimensional (2D) sample is determined by two factors. The first is related to the basic conductance swing  $\Delta G$  associated with a fluctuation in the hopping regime, which is of the order of the system conductance  $G$ . This is a characteristic feature of the strongly localized regime (which in the present case of 2D samples means sheet resistance  $R_{\square}$  that fulfills  $R_{\square} \gg \frac{\hbar}{e^2}$ ). In other words, for a system with size  $L$  smaller or equal to the scale relevant for the phenomenon observed,  $\Delta G/G$  is of the order unity.<sup>22</sup> This should be contrasted with the “universal” conductance fluctuation  $\Delta G \approx e^2/h$  characterizing the respective situation in weak localization (which holds for  $G \gg e^2/h$  and thus  $\Delta G/G \ll 1$  being the typical case). This incidentally is the main reason why CF (whether due to an interference effect or an energy-shift mechanism) and conductance noise are much more prominent in the hopping regime than they are in the diffusive one. The second factor that controls the fluctuation amplitude  $\Delta G/G$  is how many independent fluctuators the current-carrying network contains. This is essentially determined by the square root of the number of critical resistors in the sample  $N \approx \frac{LW}{\mathcal{L}^2} = \frac{A}{\mathcal{L}^2}$ , where  $\mathcal{L}$  is the percolation radius<sup>17–19</sup> and thus,  $\frac{\Delta G}{G} \approx \mathcal{L}A^{-1/2}$ . This law is depicted in Fig. 1(c) and yields  $\mathcal{L} \approx 0.3$   $\mu\text{m}$  (as can be easily seen from the figure by the extrapolated value of the best fit line to  $\frac{\Delta G}{G} \approx 1$ ). This value for the percolation radius is quite reasonable for samples with  $R_{\square}$  in the range used (and for  $T \approx 4$  K). Not surprisingly, a similar dependence on  $\mathcal{L}$  was observed for the  $1/f$ -noise magnitude.<sup>11</sup>

It should be noted that  $\mathcal{L}$  is a disorder-dependent quantity<sup>17–19</sup> and for a fixed temperature, as is the case for the data presented here, the relative amplitude of the CF (as

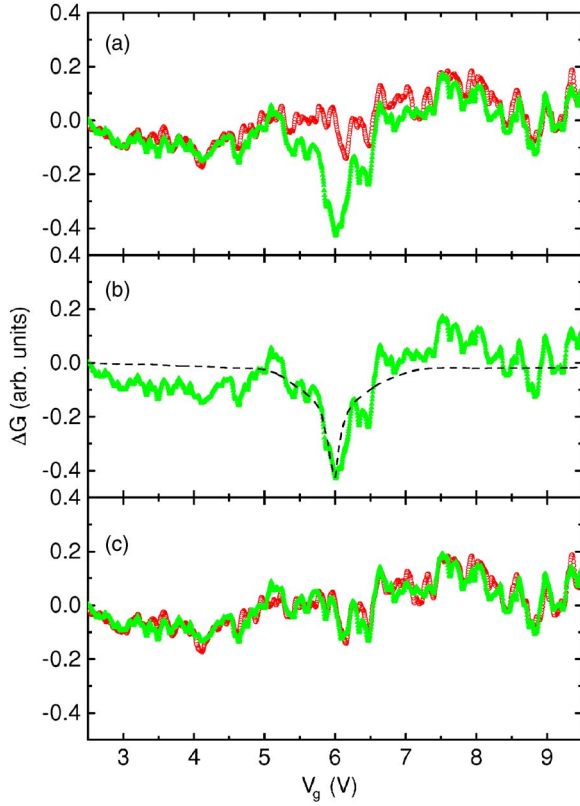


FIG. 3. (Color online) (a) The fluctuating part of several  $G(V_g)$  traces (i.e., after subtracting the equilibrium background) for a sample with  $R_{\square}=12.1 \text{ M}\Omega$ ,  $L=25 \text{ }\mu\text{m}$ ,  $W=20 \text{ }\mu\text{m}$ . The first trace was measured immediately (within  $\approx 20 \text{ s}$ ) after quench cooling the sample from  $T \approx 70 \text{ K}$  to the measurement temperature of  $4.1 \text{ K}$  (empty circles). The second trace (full triangles) was taken after the sample was allowed to equilibrate under  $V_g=6 \text{ V}$  for  $\approx 12 \text{ h}$ . The data for the latter scan are shown in (b) along with a fitted (to a Lorentzian) memory cusp (dashed line) that when subtracted from these data results in the full-triangle trace compared in (c) with the first scan. All traces were taken with a rate of  $10 \text{ mV/s}$ .

well as the  $1/f$  noise) increases with disorder. The relative amplitude of the memory cusp also increases with disorder,<sup>23</sup> making it hard to separate the electron glass from the CF phenomenon by this parameter. The features that clearly distinguish between these phenomena are the dependence on the system size and their different temporal behavior as demonstrated below.

The glassy effects seem to be simply superimposed on the CF and noise without any noticeable intermodulation between these phenomena. For example, Fig. 3 demonstrates that the reproducibility of the CF is unaffected by the presence of the memory cusp. In Fig. 3(a), we compare the  $G(V_g)$  taken immediately after cooldown with the one after the sample was allowed to relax under  $V_g=6 \text{ V}$ , which now includes a memory cusp superimposed on the CF pattern. Indeed, removing a “simulated” cusp [Fig. 3(b)] from the “relaxed”  $G(V_g)$ , the two curves show the same degree of CF registry in the voltage region where the original cusp appeared as in the regions outside it [Fig. 3(c)].

While the phenomenology associated with the CF appears to have several common features with the  $1/f$  noise, the

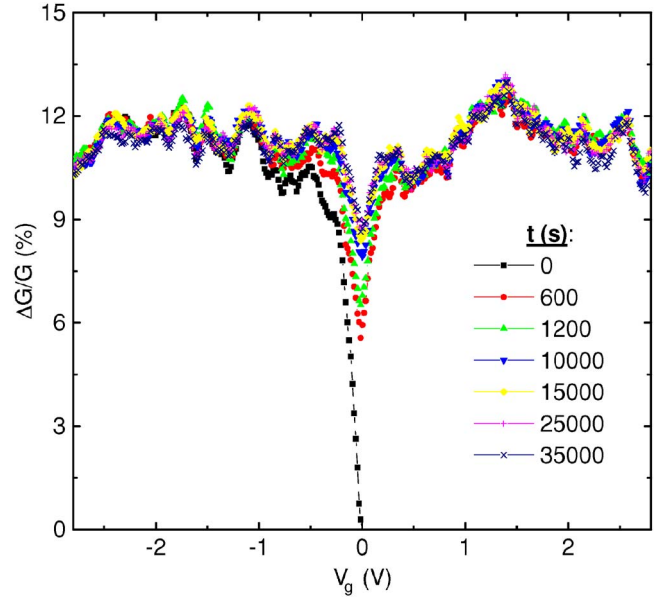


FIG. 4. (Color online)  $G(V_g)$  traces taken consecutively starting from  $V_g=0 \text{ V}$  where the sample was equilibrated for  $\approx 12 \text{ h}$ , then swept continuously in the interval  $V_g=-3 \text{ V}$  to  $V_g=+3 \text{ V}$  with a scan rate of  $10 \text{ mV/s}$ . The traces are labeled by their “age” relative to the starting time of the experiment.  $\frac{\Delta G}{G}$  is  $\frac{[G(V_g)-G_0(0)]}{G_0(0)}$ , where  $G_0$  is the equilibrium conductance. Sample parameters:  $R_{\square}=37.5 \text{ M}\Omega$ ,  $L=80 \text{ }\mu\text{m}$ ,  $W=200 \text{ }\mu\text{m}$ .

electron-glass effects seem to be controlled by a different spatial scale, and quite a different time scale. Neither the width nor the relative amplitude of the memory cusp changes when  $L$  is decreased down to the smallest scale used in our experiments. This is in contrast with the behavior of the CF and the  $1/f$  noise, which is also why the glassy effects become difficult to resolve below a certain scale. The huge disparity in the dynamics between the CF and the electron glass is illustrated by the experiment described in Fig. 4. Starting from a relaxed state at the cooldown  $V_g=V_g^o$ , multiple sweeps of the gate voltage over an interval straddling  $V_g^o$  yield  $G(V_g)$  traces that clearly show that the cusp amplitude decays with time *much* faster than the time it takes the CF pattern to change appreciably. In fact, note that for the last three to four sweeps, the amplitude of the memory cusp has already decayed to a level comparable with the amplitude of some of the wiggles associated with the CF, which appear to be fairly stationary throughout the entire experiment.

## B. Memory and dynamics

In addition to the memory cusp discussed above, essentially all the other characteristic features of the electron glass are observable in the samples that approach the mesoscopic regime. Figure 5 compares the aging behavior of an  $8 \times 18 \text{ }\mu\text{m}^2$  sample with that of a  $1 \times 1 \text{ mm}^2$  sample both using the “gate protocol”<sup>5,10,24</sup> with similar parameters and similar waiting times. The same aging protocol was used involving the following procedure. The sample is allowed to relax for  $12 \text{ h}$  at  $T=4 \text{ K}$  under a gate voltage  $V_g$  reaching a

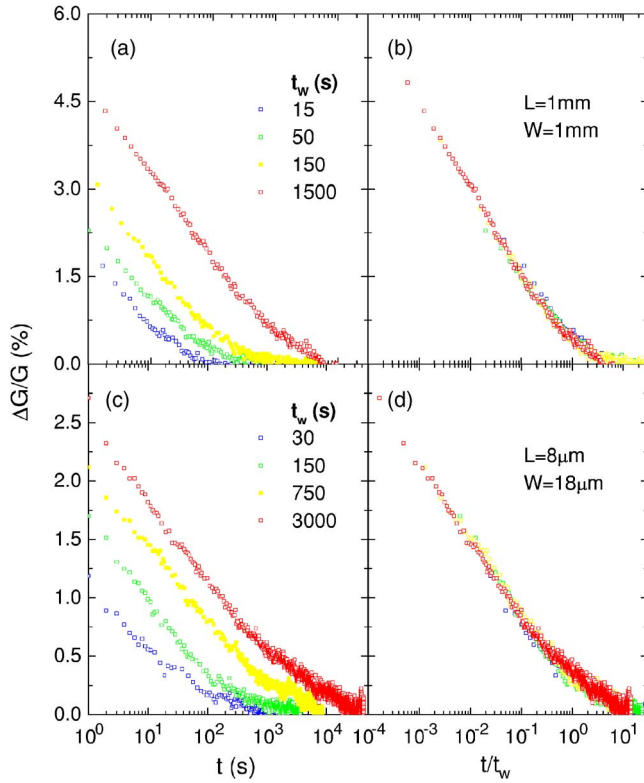


FIG. 5. (Color online) Aging experiment using the gate protocol comparing the results on the  $1 \times 1 \text{ mm}^2$  sample [(a) and (b),  $R_{\square} = 57 \text{ M}\Omega$ ], with those for  $L=8 \mu\text{m}$  and  $W=18 \mu\text{m}$  [(c) and (d),  $R_{\square} = 3.5 \text{ M}\Omega$ ]. See text for the protocol details.

near-equilibrium conductance  $G_0$  (which is used as base line for the aging protocol). Then, the gate voltage is quickly changed (typically over 5 s) from  $V_g^o$  to  $V_g^n$  and is held there for  $t_w$  after which  $V_g$  is reinstated at  $V_g^o$ . Figure 5 is a plot of the excess conductance (normalized to the equilibrium conductance  $G_0$ ) measured after  $V_g$  is set back to  $V_g^o$ . The figure shows such  $\Delta G/G$  curves as function of time for different  $t_w$  [Figs. 5(a) and 5(c)]. The same data are plotted as function of  $t/t_w$  to illustrate simple-aging behavior [Figs. 5(b) and 5(d)], which is almost identical for the “mesoscopic” and macroscopic samples. The only apparent difference is a more pronounced noise superimposed on the data of the small sample.

Down to sample sizes of  $8 \times 18 \mu\text{m}^2$ , and for the  $R_{\square}$  values used in this study (typically, 5–200 M $\Omega$  at 4 K), the amplitudes of the  $1/f$  noise and the CF were small enough, making it possible to observe a memory cusp and to perform a two-dip experiment, which is one of the better defined techniques to get a measure of the glassy dynamics.<sup>6</sup> The results of such an experiment is shown in Fig. 6. Note that the characteristic relaxation time  $\tau$ , as defined by the two-dip experiment, for this sample [Fig. 6(b)] is of the order of  $10^3$  s. This is quite similar to the values typically obtained for samples of  $\text{In}_2\text{O}_{3-x}$  of millimeter size,<sup>3</sup> which means that down to  $\approx 10 \mu\text{m}$  the dynamics does not change from its macroscopic value. Unfortunately, it was not feasible to perform a two-dip experiment on smaller samples because the magnitude of the CF became larger than the modulation associated with the memory cusp.

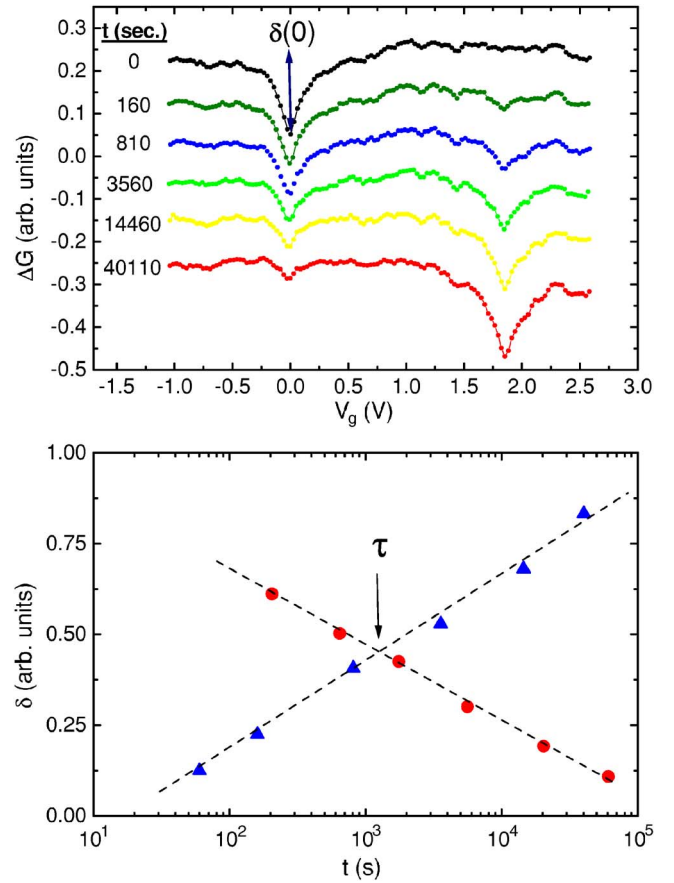


FIG. 6. (Color online) Two-dip experiment with a  $L=8 \mu\text{m}$ ,  $W=18 \mu\text{m}$  sample ( $R_{\square} = 55 \text{ M}\Omega$ ). The top graph shows  $G(V_g)$  traces taken at different times; starting from equilibrated position under  $V_g^o = 0 \text{ V}$ , an initial scan is taken showing a well developed memory cusp at this  $V_g$ . The gate voltage is then swept to and parked at  $V_g^n = 1.85 \text{ V}$  for the rest of the experiment and  $G(V_g)$  traces taken at later times as indicated (traces are displaced along the ordinate for clarity). Note the appearance of a new memory cusp at  $V_g^n$  becoming more prominent with time, while the visibility of the old cusp at the original equilibration voltage  $V_g^o$  decreases with time. Scan rate for all traces was 10 mV/s. The bottom graph shows the decay of the amplitude for the old cusp (circles) and the buildup of memory-cusp amplitude at the new gate-voltage position (triangles). Amplitudes are measured relative to the “natural” background of  $G(V_g)$ .

To be able to make a systematic study of the dependence of glassy dynamics on sample size including samples smaller than  $10 \mu\text{m}$ , we resorted to the “single-conductance-excitation” method. This is based, as a first step, on monitoring the relaxation of the excess conductance created, e.g., by a  $V_g$  switch from  $V_g^o$  to  $V_g^n$ . The excess conductance follows the logarithmic law:<sup>5,10</sup>

$$\Delta G(t) = \Delta G(t_0) - a \log(t/t_0), \quad (1)$$

where  $\Delta G(t_0)$  is the initial amplitude of the excess conductance attained, just after  $V_g$  is switched to  $V_g^n$  (within the experiment resolution time  $t_0$ , typically 1 s). Conductance relaxation curves exhibiting the logarithmic law for sample

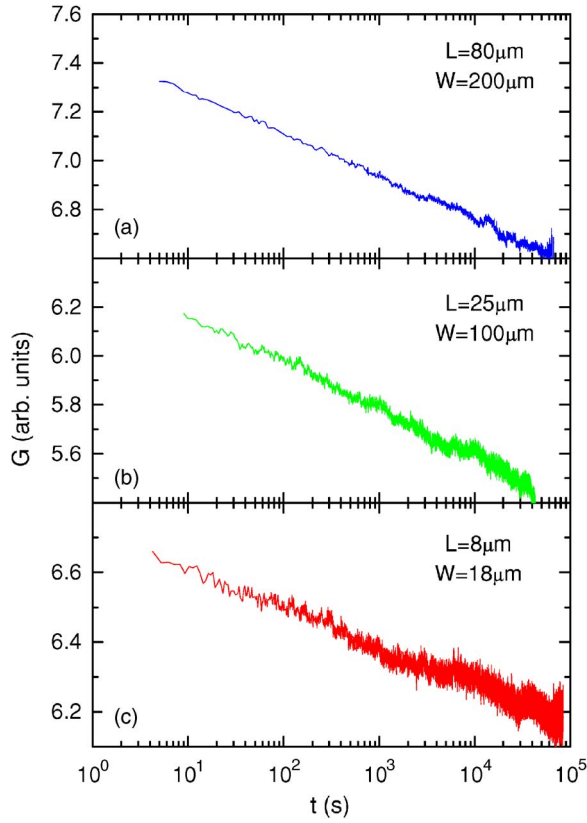


FIG. 7. (Color online) Relaxation of the sample conductance following an excitation by switching the gate voltage from a  $V_g^o$  at which the sample was equilibrated to  $V_g^n$  (the typical swing of  $V_g$  used in these experiments  $|V_g^o - V_g^n|$  was in the range 2–10 V). Data are shown for samples with different lateral dimensions as indicated and with  $R_{\square}$  of 35.5, 69.2, and 175 M $\Omega$  for the sample in (a), (b), and (c), respectively.

sizes down to  $8 \times 18 \mu\text{m}^2$  are illustrated in Fig. 7. The systematic increase of noise as the sample dimension is reduced is clearly reflected from this figure yet the  $\log(t)$  law is reasonably well defined in these samples and may be used to get a measure of dynamics as explained below. For the  $2 \times 2 \mu\text{m}^2$  samples, however, the  $1/f$ -noise amplitude is often larger than  $\Delta G(t_0)$  and the relaxation process may be obscured to the degree that even the sign of  $\partial[\Delta G(t)]/\partial t$  is in doubt. The noise for a typical  $2 \times 2 \mu\text{m}^2$  sample is shown in Fig. 8, and in the time trace one can see time periods during which the conductance may drift in either direction from its mean value by 2%–4%, which is comparable to the  $\Delta G(t_0)$  associated with (macroscopic) samples with similar parameters.<sup>10</sup> Due to the  $\log(t)$  law, over  $10^2$ – $10^3$  s a substantial part of  $\Delta G$  dies out, and therefore even the sign of  $\Delta G$  versus  $t$  becomes difficult to ascertain in this situation. Two relaxation curves illustrating this unwieldy behavior of  $\Delta G(t)$  for typical single runs of small sample are shown in Figs. 9(a) and 9(b). Apparently, the only way to get a more manageable  $\Delta G(t)$  in this realm of sample size is to use averaging. Figure 9(c) shows the relaxation curve for the same  $2 \times 2 \mu\text{m}^2$  sample averaged over 53 individual runs that were acquired by performing multiple excitation-relaxation runs. This was realized by using two end points

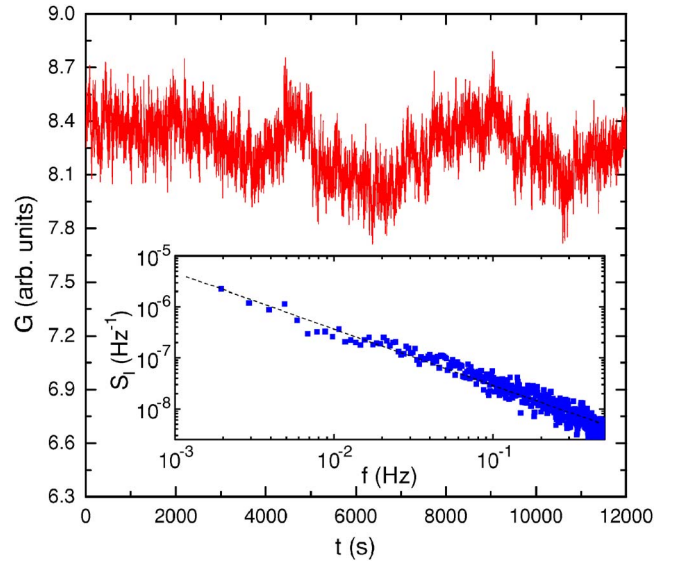


FIG. 8. (Color online) Conductance versus time (at equilibrium) for a sample with  $2 \times 2 \mu\text{m}^2$  lateral dimensions and with  $R_{\square}$  of 56 M $\Omega$ . Note the accentuated noise level. The inset shows the power spectrum averaged over 14 time traces each 1024 s. long. The dashed line is a best fit to  $1/f^\alpha$  law ( $\alpha \approx 1.15$ ).

for  $V_g$  along the gate-voltage range, and monitor the relaxation of  $G$  at each end point for a time  $t^*$  after  $V_g$  was switched from the other end point. The two end points  $V_g^1$  and  $V_g^2$  were chosen to be far enough from one another such that the voltage swing  $|V_g^1 - V_g^2|$  was considerably bigger than the width of the memory cusp to minimize history effects.<sup>10</sup> For the same reason, the data used in Fig. 9 are limited to time spans smaller than  $t^*$ . The resulting relaxation curve [Fig. 9(c)], except for being still much more noisy, is quite similar to the relaxation curves of the larger samples in that it follows the logarithmic law, and with similar dynamics as is shown next.

To extract a measure of the dynamics from the  $G(t)$  curves such as in Figs. 7 and 9, one needs first to subtract the equilibrium value of  $G$ , then take into account the equilibrium field effect  $\Delta G_{eq}$ . The latter is the change in  $G$  due to the change in the thermodynamic density of states associated with the  $V_g^o \rightarrow V_g^n$  switch.<sup>25</sup> The value of  $\Delta G_{eq}$  is estimated separately for each sample using the antisymmetric part of the field effect (see Ref. 25 for details). Then, normalizing by  $\Delta G(t_0)$  yields a logarithmic curve for  $\Delta G(t)$  with the boundary condition  $\Delta G(t_0) \equiv 1$  from which a relaxation rate for  $\Delta G$  is obtained as percent change per time decade. With the above normalization, this value is a proper measure of the system dynamics in that it allows comparison between different samples and/or different conditions of measurement. Figure 10 summarizes the results of this procedure for samples with sizes ranging from  $1 \times 1 \text{ mm}^2$  to  $2 \times 2 \mu\text{m}^2$ , all tested at  $T=4.1$  K and having similar resistances.

In principle, a similar averaging stratagem as that described above to deal with the  $1/f$ -noise problem may be employed to facilitate the observation of the memory cusp in small samples. This would entail averaging over data obtained in many quench-cooling events, each followed by a

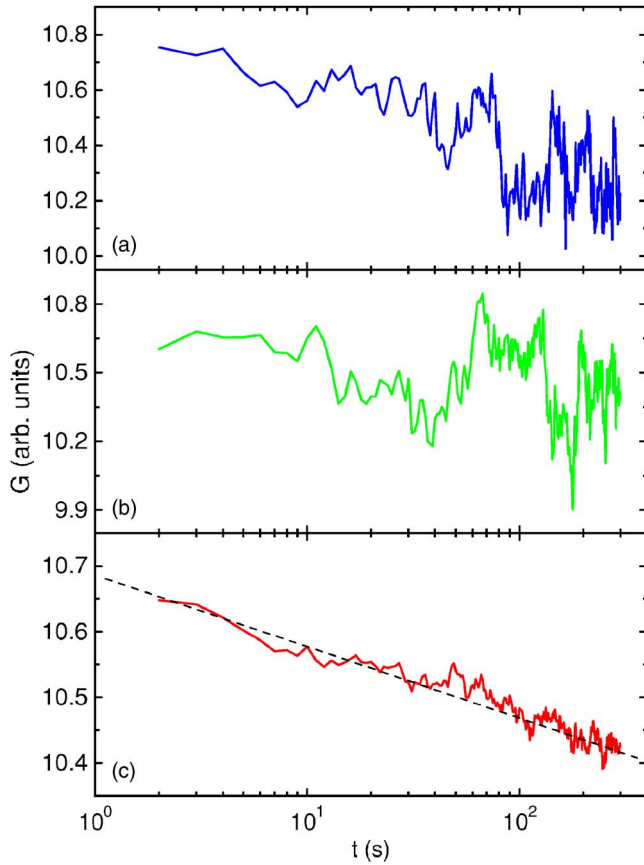


FIG. 9. (Color online) Relaxation of the sample conductance following an excitation by switching the gate voltage from a  $V_g^o = -7$  V at which the sample was equilibrated to  $V_g^n = +7$  V for the same sample as in Figs. 8(a) and 8(b) which are two typical single runs, while (c) is the result of averaging over 53 such traces that were obtained by alternate switching between  $V_g^o$  and  $V_g^n$  (see text for details).

long period of relaxation (to build up the cusp). Such a procedure, however, is prone to sample damage in addition to being prohibitively time consuming.

To summarize, we have shown in this work that the dynamics of the electron glass has a different time and spatial scale than those associated with the mesoscopic conductance fluctuations. These conclusions are inferred from the following experimental results.

(1) The CF pattern is fully developed immediately after cooling the sample, while the memory-cusp amplitude takes many hours to build.

(2) Starting from a cold and well-equilibrated sample, continuously sweeping  $V_g$  causes the memory-cusp amplitude to diminish with a typical time scale of hours, while the CF visibility remains essentially intact for many days.

(3) Thermally cycling the sample creates a different pattern of CF, while the shape and relative magnitude of the memory cusp is the same (as long as the average conductance of a given sample is the same).

Inasmuch as the CF pattern is taken as a snapshot of the underlying potential landscape, these findings seem to indicate that the electron-glass dynamics may be treated as essentially independent of the lattice dynamics although in

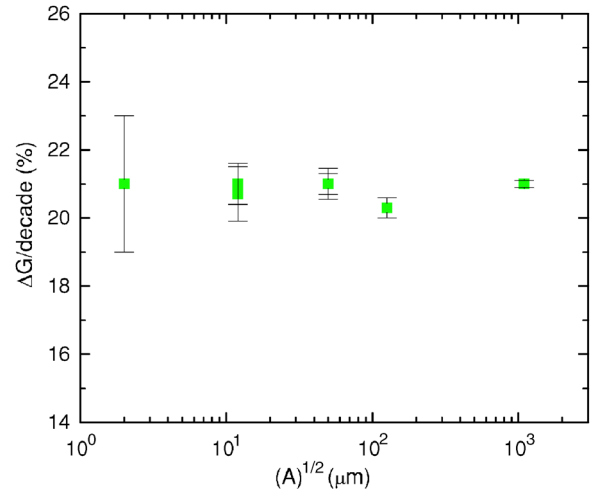


FIG. 10. (Color online) The relaxation rate of the excess conductance produced as in Figs. 7 and 8 for samples with various sizes and with similar values of  $R_{\square}$ , all measured at  $T=4.1$  K.

terms of energy exchange (and dissipation) the two systems are coupled. This is not a trivial result as there is no reason to assume that the lattice potential is stationary over the time scale relevant for the electron glass. In fact, ions, atoms, and perhaps group of atoms are presumably mobile even at cryogenic temperatures, thus producing potential fluctuations.<sup>26</sup> These are believed to be the main source of the  $1/f$  noise which includes time scales that overlap those typical of the electron-glass dynamics. It is therefore plausible to expect that the two phenomena affect one another to some degree. For example, one intuitively expects that the conductance noise will be modified when the system is relaxing from an excited state (or, more generally, when it is out of equilibrium). In the present case, however, where  $\Delta G$  in the excited state is typically few percents of the equilibrium conductance, this seems to be a small effect that so far escaped our detection.<sup>27</sup> An attempt to find a change in the  $1/f$ -noise characteristics when the system is deliberately taken out of equilibrium yielded a null result. Such an experiment was carried out by keeping the sample in an excited state for a sufficiently long time to allow adequate averaging of the noise spectrum.<sup>28</sup> This steady-state, out-of-equilibrium situation was achieved by a continuous sweep of the gate voltage over a certain voltage interval. Data for  $G(t)$  were taken after the memory cusp was erased by allowing this process to proceed for two days. The noise characteristics were compared with those taken with a fixed-gate situation for which data were taken after the sample was allowed to relax (and build a memory cusp). In either case, the noise spectrum was obtained by Fourier transforming 25 conductance time traces each composed of 1024 points taken with 1 s resolution. It turns out that, within the error of the procedure, the  $1/f$ -noise magnitude and spectrum were essentially the same for the “near-equilibrium” and the “excited” sample. Full details of this experiment as well as the implications to the general issue of flicker noise in the hopping regime will be given elsewhere.<sup>29</sup>

Finally, throughout the size range where the memory cusp could be resolved over the background of the CF and the  $1/f$

noise, its amplitude and characteristic width do not depend on sample size. Likewise, the dynamics associated with conductance relaxation is independent of sample size down to  $2\ \mu\text{m}$ . These findings suggest that the relevant length scale for the electron glass is considerably smaller than the sample sizes used in this study.

## ACKNOWLEDGMENTS

The authors are grateful for useful discussion with A. Efros and M. Pollak. This research was supported by a grant administered by the US Israel Binational Science Foundation and by the Israeli Foundation for Sciences and Humanities.

- 
- <sup>1</sup>M. Ben-Chorin, Z. Ovadyahu, and M. Pollak, *Phys. Rev. B* **48**, 15025 (1993).
- <sup>2</sup>G. Martinez-Arizala, D. E. Grupp, C. Christiansen, A. M. Mack, N. Markovic, Y. Seguchi, and A. M. Goldman, *Phys. Rev. Lett.* **78**, 1130 (1997); G. Martinez-Arizala, C. Christiansen, D. E. Grupp, N. Markovic, A. M. Mack, and A. M. Goldman, *Phys. Rev. B* **57**, R670 (1998).
- <sup>3</sup>Z. Ovadyahu and M. Pollak, *Phys. Rev. Lett.* **79**, 459 (1997).
- <sup>4</sup>T. Grenet, *Eur. Phys. J. B* **32**, 275 (2003).
- <sup>5</sup>A. Vaknin, Z. Ovadyahu, and M. Pollak, *Phys. Rev. B* **65**, 134208 (2002).
- <sup>6</sup>A. Vaknin, Z. Ovadyahu, and M. Pollak, *Phys. Rev. Lett.* **81**, 669 (1998).
- <sup>7</sup>M. Müller and L. B. Ioffe, *Phys. Rev. Lett.* **93**, 256403 (2004).
- <sup>8</sup>Sh. Kogan, *Phys. Rev. B* **57**, 9736 (1998).
- <sup>9</sup>T. Kawasaki and S. Miyashita, *J. Magn. Magn. Mater.* **104**, 1595 (1992); A. Bunde, S. Havlin, J. Klafter, G. Graff, and A. Shehter, *Phys. Rev. Lett.* **78**, 3338 (1997); Andrea Montanari and Guilhem Semerjian, *J. Stat. Phys.* **125**, 23 (2006).
- <sup>10</sup>Z. Ovadyahu and M. Pollak, *Phys. Rev. B* **68**, 184204 (2003).
- <sup>11</sup>V. Orlyanchik, V. I. Kozub, and Z. Ovadyahu, *Phys. Rev. B* **74**, 235206 (2006).
- <sup>12</sup>S. Washburn and R. A. Webb, *Rep. Prog. Phys.* **55**, 1311 (1992), and references therein.
- <sup>13</sup>W. J. Skocpol, P. M. Mankiewich, R. E. Howard, L. D. Jackel, D. M. Tennant, and A. D. Stone, *Phys. Rev. Lett.* **56**, 2865 (1986).
- <sup>14</sup>P. A. Lee, *Phys. Rev. Lett.* **53**, 2042 (1984).
- <sup>15</sup>A. B. Fowler, A. Hartstein, and R. A. Webb, *Phys. Rev. Lett.* **48**, 196 (1982); W. J. Skocpol, L. D. Jackel, E. L. Hu, R. E. Howard, and L. A. Fetter, *ibid.* **49**, 951 (1982); R. F. Kwasnick, M. A. Kastner, J. Melngailis, and P. A. Lee, *ibid.* **52**, 224 (1984).
- <sup>16</sup>O. Faran and Z. Ovadyahu, *Phys. Rev. B* **38**, 5457 (1988); *Solid State Commun.* **67**, 823 (1988); D. Shahar and Z. Ovadyahu, *Phys. Rev. Lett.* **64**, 2293 (1990).
- <sup>17</sup>B. I. Shklovskii and A. L. Efros, *Sov. Phys. JETP* **33**, 468 (1971).
- <sup>18</sup>M. Pollak, *J. Non-Cryst. Solids* **11**, 1 (1972).
- <sup>19</sup>V. Ambegaokar, B. I. Halperin, and J. S. Langer, *Phys. Rev. B* **4**, 2612 (1971).
- <sup>20</sup>A. Miller and E. Abrahams, *Phys. Rev.* **120**, 745 (1960).
- <sup>21</sup>P. A. Lee and A. D. Stone, *Phys. Rev. Lett.* **55**, 1622 (1985); S. Feng, P. A. Lee, and A. D. Stone, *ibid.* **56**, 1960 (1986).
- <sup>22</sup>Y. Imry, *Europhys. Lett.* **1**, 249 (1986); F. P. Milliken and Z. Ovadyahu, *Phys. Rev. Lett.* **65**, 911 (1990); Z. Ovadyahu, *Waves Random Media* **9**, 241 (1999), and references therein.
- <sup>23</sup>M. Pollak and Z. Ovadyahu, *J. Phys. I* **7**, 1595 (1997).
- <sup>24</sup>A. Vaknin, Z. Ovadyahu, and M. Pollak, *Phys. Rev. Lett.* **84**, 3402 (2000).
- <sup>25</sup>Z. Ovadyahu, *Phys. Rev. B* **73**, 214208 (2006).
- <sup>26</sup>Movements of these objects, commonly referred to as two-state systems, may be triggered by electronic transitions such as changes in bonding angle. Therefore, these are as much “electronic” as they are “atomic.” The only distinction we make is based on whether the objects actually contribute to macroscopic dc current or just modulate it. The possible role of ion movement and its relation to the electron-glass dynamics were discussed before *vis-a-vis* the dependence of the dynamics on disorder and magnetic field (Ref. 3).
- <sup>27</sup>Note that renormalization of hopping rates due to the coupling of electrons to two-state systems may still be at work and that may affect, e.g., the relaxation rate of  $\Delta G$ . This issue is now under study.
- <sup>28</sup>The relaxation of  $\Delta G$  in a “one-shot” experiment (as, for example, in Fig. 7) leaves very little time for a measurement of  $1/f$  noise while the system is in the “excited” state; due to the logarithmic law, most of the excess conductance (which is small anyhow relative to the equilibrium value) is gone by  $\Delta t \approx 100\text{--}500$  s.
- <sup>29</sup>Z. Ovadyahu (unpublished).